Performance evaluation of IR-UWB in short-range fiber communication using linear combination of monocycles

Citation for published version (APA):
Abraha, S. T., Okonkwo, C. M., Yang, H., Visani, D., Shi, Y., Jung, H. D., ... Koonen, A. M. J. (2011). Performance evaluation of IR-UWB in short-range fiber communication using linear combination of monocycles. Journal of Lightwave Technology, 29(8), 1143-1151. DOI: 10.1109/JLT.2011.2120595

DOI:
10.1109/JLT.2011.2120595

Document status and date:
Published: 01/01/2011

Document Version:
Publisher's PDF, also known as Version of Record (includes final page, issue and volume numbers)

Performance Evaluation of IR-UWB in Short-Range Fiber Communication Using Linear Combination of Monocycles

Solomon Tesfay Abraha, *Student Member, IEEE*, Chigo Okonkwo, *Member, IEEE*, Hejie Yang, *Student Member, IEEE*, Davide Visani, *Student Member, IEEE*, Yan Shi, *Student Member, IEEE*, Hyun-Do Jung, *Member, IEEE*, Eduward Tangdiongga, *Member, IEEE*, and Ton Koonen, *Fellow, IEEE*

***Abstract*—We present the performance evaluation of impulse radio ultrawideband (IR-UWB) over fiber using a simple pulse design technique with a high fractional bandwidth. The technique, based on the linear combination of the first-order Gaussian derivatives with different pulse-shaping factors, shows full compliance with Federal Communications Commission mask requirements even in the most severely power-restricted GPS band. We validated our approach with experiments employing an intensity-modulation direct-detection scheme. The experimental setup uses a directly modulated DFB laser at 1302.56 nm and a multimode fiber-coupled photodetector with 24 μm diameter photosensitive area. The transmission link consists of 25 km single-mode fiber or 4.4 km multimode fiber. Error-free transmission at 2 Gb/s is achieved over both fiber links. The result shows the proposed pulse-generation technique to be simple and cost-effective compared to higher order Gaussian derivative schemes. This can be implemented successfully to distribute UWB signals over optical links for access and in-building networks.**

***Index Terms*—Impulse radio (IR), in-building network, signal processing, ultrawideband (UWB) communications.**

I. Introduction

In recent years, ultrawideband (UWB) technology has been considered as one of the most promising techniques for next generation short-range broadband wireless communications and sensor networks. The growing interest in this technique is due to its many abilities: low cost, high data capacity, low power consumption, coexistence with other wireless services, enhanced robustness against multipath fading, low probability of interception, and ability to pass through walls while maintaining communication [1], [2]. However, the main limitation of a UWB system is the limited propagation distance (typically $<$10 m) over which the expected high data rate can be realized. This is mainly due to low power spectral density (PSD) assigned to -41.3 dB·m/MHz in the frequency range from 3.1–10.6 GHz regulated by the FCC. To increase the coverage area, UWB signals can be distributed over wired lines such as coaxial cable or optical fiber. Due to the low loss, large bandwidth and immunity to electromagnetic interference, inherent to optical fiber, UWB over fiber is considered a promising solution [3].

A carrier-free impulse radio ultrawideband (IR-UWB) system is an approach to UWB systems based on the radiation of waveforms formed by sequences of very short duration pulses of the order of hundreds of picoseconds. The information to be transferred is usually represented in digital form by a binary sequence and each bit is transferred using one or more pulses that are directly radiated for base-band air transmission [4]. Therefore, by avoiding a complex tunable frequency mixer, intermediate frequency carrier and filter circuits, the transmitter is simplified and hence greatly reduce the cost. Moreover, it has good pass-through performance due to the base-band transmission and much more suitable for indoor wireless communications and localization [5]. This feature makes IR-UWB unique compared to multiband orthogonal frequency division multiplexing UWB scheme; hence, it can also be combined with radio array beam forming, leading to a power-efficient short-range wireless communications.

One of the fundamental points that require detailed consideration in IR-UWB circuits and systems design is the selection of the impulse signal type as it determines the performance of the IR-UWB system. The techniques for generating IR-UWB pulses can be classified into two main categories: electrical- and photonic-generation techniques. In both generation techniques, Gaussian-based monocycle pulses and doublets are considered as conventional pulses due to better bit error rates (BERs) and robust multipath resilience as compared to different impulse signals [6]. However, they do not fully satisfy the FCC-mask requirements with good power efficiency, and hence, different pulse design techniques in the electrical domain have been proposed [7]–[12]. A review of different pulse design techniques is provided in [13].

In the past few years, several photonic-generation schemes that focused on the generation of conventional monocycle and doublet employing different schemes have been reported [14]–[23]. Recently, photonic-generation techniques that focused on generation of nonconventional pulses with aim at

Manuscript received July 21, 2010; revised December 11, 2010; accepted February 20, 2011. Date of publication February 28, 2011; date of current version April 01, 2011. This work was supported by the EU program FP7 ICT-212352 ALPHA.

S. T. Abraha, C. Okonkwo, H. Yang, Y. Shi, E. Tangdiongga, and T. Koonen are with the COBRA Research Institute, Technical University of Eindhoven, Eindhoven 5612 AZ, The Netherlands (e-mail: s.t.abraha@tue.nl; c.m.okonkwo@tue.nl; h.yang1@tue.nl; y.shi@tue.nl; e.tangdiongga@tue.nl; a.m.j.koonen@tue.nl).

D. Visani is with the Dipartimento di Elettronica Informatica e Sistemistica (DEIS), University of Bologna, Bologna 40136, Italy (e-mail: davide.visani3@unibo.it).

H.-D. Jung is with Bell Labs Seoul, Alcatel-Lucent, Seoul 120-270, Korea (e-mail: jhd94@ieee.org).

Color versions of one or more of the figures in this paper are available online at http://ieeexplore.ieee.org.

Digital Object Identifier 10.1109/JLT.2011.2120595

enhancing the power efficiency have been reported [24]–[28]. However, previously proposed photonic-generation techniques are complex and expensive, especially for short-range fiber communications such as in in-building networks.

In this paper, we propose a simple and new electrical pulse-generation concept that can reduce complexity and cost of the system. Our concept is based on linear combination of two monocycles with different pulse-shaping factors. By this process, the proposed pulse has more zero crossings in the temporal response, leading to a more power-efficient and fully FCC-compliant pulse even in the most severely power-restricted GPS band from 0.96 to 1.61 GHz. This proposed approach has been simulated and experimentally demonstrated.

The paper is organized as follows. After the introduction in Section I , the conventional pulse design approach and limitations are discussed in Section II . The proposed pulse design principle is discussed in Section III . Section IV summarizes the key features of the proposed pulse compare to conventional pulses. Section V presents experimental setup in detail. In Section VI, detailed experimental results of 2 Gb/s IR-UWB over 25 km single-mode fiber (SMF) and 4.4 km multimode fiber (MMF) are presented. Finally, the paper is concluded in Section VII.

II. Conventional Pulse Design Approach and Limitations

UWB systems are power-limited systems rather than spectral limited. Therefore, waveform design for the IR-UWB communication is a major issue and the aim is to obtain a pulse waveform that complies with FCC mask as closely as possible and maximize the bandwidth as well [8]. A typical signal that can be considered as a basis function for IR-UWB transmission is the Gaussian pulse expressed as

$$x(t) = \frac{A}{\sqrt{2\pi\sigma^2}} e^{\left(-\frac{t^2}{2\sigma^2}\right)} \quad (1)$$

where A and σ denote the amplitude and spread or shaping factor of the Gaussian pulses, respectively. As antennas are not efficient at DC, it is preferable to use derivatives of Gaussian pulse that have smaller DC components. Accordingly, in the UWB systems, the most commonly used waveforms are monocycle and doublet. These pulses are becoming conventional and most widely used in photonic generation of UWB over fiber due to the mathematical simplicity, multipath resilience, and good BER performance [14]–[23].

On the other hand, these commonly used pulses do not satisfy the requirement of the FCC mask with high power efficiency. The PSD of *n*th derivative of Gaussian pulse can be obtained recursively as provided in [7]–[9]. It is obvious that everything can fit FCC mask if the power is low enough. However, as UWB is a power-limited system, the radiating power must be as high as possible without violating the regulation. Therefore, in Fig. 1, we use the first seven derivatives of the Gaussian pulse with an optimal pulse-shaping factor for each derivative to make the spectrum as wide as possible. Then, PSD of each derivative is normalized and finally scaled to the maximum legally allowed PSD. Notice that the low-order derivatives $(n \leq 4)$ are not FCC compliant around the GPS band if they are

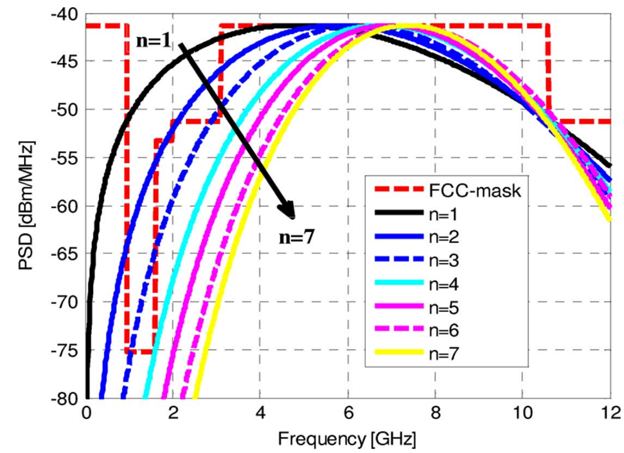

Fig. 1. PSD of higher order derivatives of Gaussian pulse.

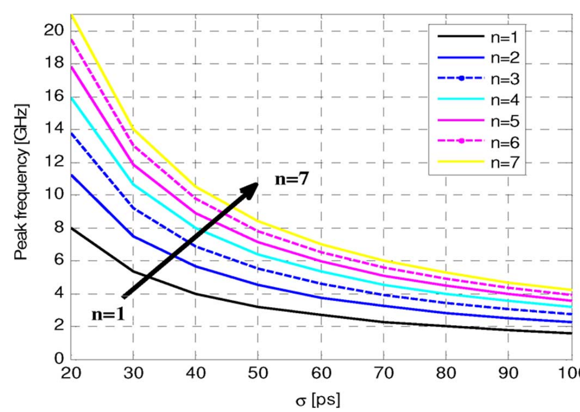

Fig. 2. Peak frequency versus pulse-shaping factor σ [ps].

forced to optimize the assigned power and the bandwidth. The main reason for this limitation is that most of their energy or peak frequency lies in the low-frequency range. Therefore, in order to respect the FCC-mask regulations, higher order derivatives are preferable because the peak frequency of the pulse is increased with increasing derivation order as shown in Fig. 1. Accordingly, a fifth-order derivative is recommended in [10]. However, it is more complex and not suited for short-range fiber communications.

A general relationship between peak frequency f_{peak}, the order of derivation k and the shaping factor σ [ps] by observing the Fourier transform of the kth derivative is given by [4]

$$f_{\text{peak}} = \sqrt{k}\frac{1}{\sigma\sqrt{\pi}}. \quad (2)$$

Variation of peak frequency with pulse-shaping factor σ for the first seven derivatives of the Gaussian pulse is shown in Fig. 2. According to the simulation result shown in Fig. 2, the smaller pulse shaping factors the higher peak frequency. Furthermore, the bandwidth of the signal increases as the pulse-shaping factor becomes smaller due to the time and bandwidth inverse relationship. In general, differentiation of the Gaussian pulse influences the PSD; both peak frequency and the bandwidth of the pulse vary with differentiation order and pulse-shaping factor. Therefore, as the order of the derivatives increases, the energy of the pulse moves to higher frequency bands and thus the allocated spectrum is used more efficiently.

In general, the main bottleneck of UWB remote communication is due to electromagnetic interference between UWB systems and the GPS band. The FCC-mask requirement for protecting the GPS band and the low peak frequency of the conventional pulses lead them to be power-inefficient pulses. Furthermore, it is very important to note that IR-UWB systems for applications in consumer electronics or short-range fiber communications required low complexity, low cost, low power consumption, high power efficiency, and high data rate. Therefore, an IR-UWB pulse design technique must consider both the FCC-mask and the system requirements. All previously reported [7]–[13] electrical IR-UWB pulse design techniques do not satisfy all the requirements. Hence, a new pulse design approach is required to satisfy all the requirements and also exploits the simplicity, achievability, and good BER performance of conventional pulses by using signal-processing techniques.

III. Proposed Pulse Design Technique

In general, shaping the spectrum by modifying the pulse waveform is an interesting feature of IR-UWB. Basically, the spectrum may be shaped in three different ways: pulsewidth variation, pulse derivation, and combination of base functions. In order to reduce the complexity of the systems, we consider a linear combination of two first-order derivatives of Gaussian pulses called monocycles using different pulse-shaping values of σ_{11} and σ_{12} . The linear sum value $y_{ws1}(t)$ is given by

$$y_{ws1}(t) = a_{11}x_{11}(t,\sigma_{11}) + a_{12}x_{12}(t,\sigma_{12}) \quad (3)$$

where $x_{1i}(t,\sigma_{1i})$ is the first-order derivatives of Gaussian pulses, expressed by [7]

$$x_{1i}(t,\sigma_{1i}) = \left[\frac{-2t}{\sigma_{1i}^2}\right] \exp\left(\frac{-t^2}{2\sigma_{1i}^2}\right) \quad (4)$$

with $i = 1,2$; $\sigma_{11} = 81.35$ ps and $\sigma_{12} = 50.3$ ps are the pulse-shaping factors used for each monocycles. Furthermore, $a_{11} = 0.81$ and $a_{12} = -1.2$ are the normalized optimal weighting parameters used for our experiment. In practice, the summation of the pulses can be realized by a wideband RF power splitter and combiner that have a flat frequency response in the desired band. In the optimization of the IR-UWB pulse weighting parameters, two searching criterions were used. First, the generated RF spectrum must be fully FCC compliant; the test pass parameter ξ can be defined as

$$\xi = \begin{cases} 1, & \min\{P_{\text{FCC}}(f) - Y(f)\} \geq 0, \forall f \in [0, f_{\max}] \\ 0, & \text{otherwise} \end{cases} \quad (5)$$

where $\mathrm{P_{FCC}}(f)$ is the FCC spectral density mask and $\mathrm{Y}(f)$ is the PSD of the pulse, respectively. The value of the test parameter, $\xi = 1$, indicates the compliance of the PSD of the pulse with FCC-mask requirements otherwise $\xi = 0$ indicates violation of the FCC mask. The maximum frequency $f_{\max}$ considered during the simulation is 12 GHz.

Second, as IR-UWB systems are power-limited systems, the power efficiency of the pulse within the useful UWB band should be as high as possible. Hence, the power efficiency η is defined as the ratio between the average power of the pulse within the useful UWB band (3.1–10.6 GHz) and the total admissible power under the FCC mask within the same band which must be maximized. It is expressed as

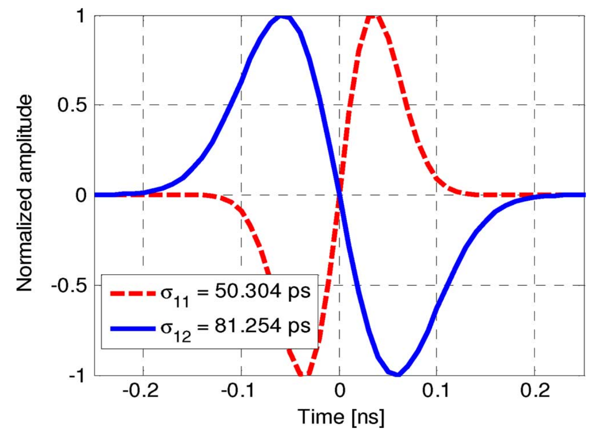

Fig. 3. Two monocycles with different pulse-shaping factors.

$$\eta = \frac{\int_{f_l=3.1\text{ GHz}}^{f_h=10.6\text{ GHz}} Y(f)df}{\int_{f_l=3.1\text{ GHz}}^{f_h=10.6\text{ GHz}} P_{\text{FCC}}(f)df} \times 100\%. \quad (6)$$

Maximizing the power efficiency yields that the bandwidth of the pulse at -10 dB as defined by FCC as large as possible. This in turn helps to achieve high data rates and hence increase spectral efficiency of the system. Therefore, the pulse-shaping parameters $\boldsymbol{\sigma_{11}}$ and $\boldsymbol{\sigma_{12}}$ mainly determine the bandwidth of the pulse and are selected based on the peak frequency and pulse-shaping factor relationship provided in (2). Then, the weighting factors are determined in such a way that the FCC-mask requirement as represented in (5) is satisfied as well as optimizing the power efficiency [as provided in (6)].

The Fourier transform of $y_{ws1}(t)$ is given by

$$Y_{ws1}(f) = a_{11}X_{11}(f,\sigma_{11}) + a_{12}X_{12}(f,\sigma_{12}) \quad (7)$$

where

$$X_{1i}(f,\sigma_{1i}) = (j2\pi f)\exp\left(-\frac{(2\pi f\sigma_{1i})^2}{2}\right). \quad (8)$$

The simulation result of each normalized monocycle pulse is shown in Fig. 3 . The normalized pulse after linear combinations of the pulses using their corresponding weighting coefficient is depicted in Fig. 4 and its corresponding spectral density compared with FCC mask is shown in Fig. 5. According to the simulation result shown in Fig. 5, we observe that the newly designed IR-UWB pulse fits the FCC mask better than the conventional monocycle and doublet pulses even in the power-restricted GPS band from 0.96 to 1.61 GHz. Furthermore, due to the side lobes created in the basic shape of the monocycle, the designed pulse has more zero crossings compared to the conventional monocycle and doublet pulse, which moves the energy of the pulse

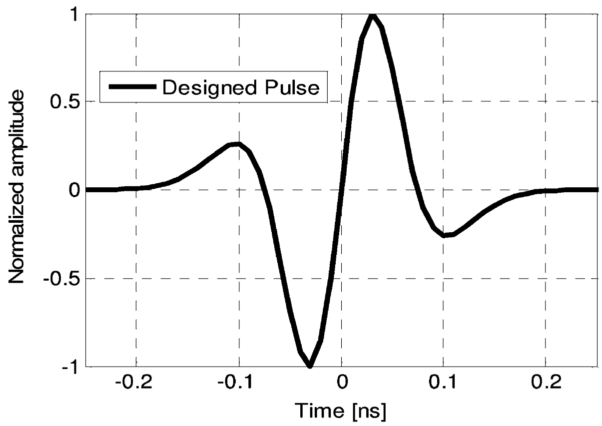

Fig. 4. Designed pulse after linear combination.

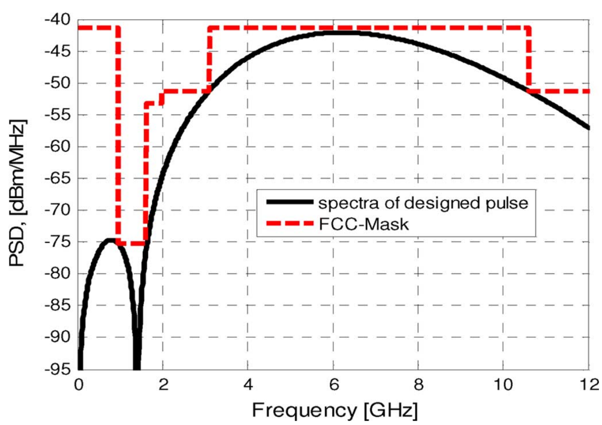

Fig. 5. PSD of higher order derivatives of Gaussian pulse.

to higher frequency ranges with similar effect as higher derivatives of Gaussian pulse. Accordingly, the resulted pulse has a central frequency of 6 GHz and a 10 dB bandwidth of 7.5 GHz with fractional bandwidth of 125% as shown in Fig. 5. Note that antenna response is an important factor as reported in [25], [26]. However, different antenna type and different antenna configuration yields different characteristics. Hence, in this paper, we present a generic approach to design a pulse that confirms the FCC-mask requirement with high power efficiency by assuming an antenna with flat gain and a linear phase response in the desired band. An antenna with reasonably quite flat response in the desired UWB band is commercially available (Skycross SMT-3TO10M-A) and it has been reported in [29]. Hence, the novelty of this approach lies in employing a linear combination of the lowest derivative of Gaussian pulses in order to provide all the desired features needed for UWB communication systems especially for short-range fiber communications.

IV. Features of Proposed Approach

A. Simplicity and Cost

To fit the FCC mask with good power efficiency, a fifth-order derivative in electrical domain was recommended in [10]. However, as the order of derivative of Gaussian pulse increases, the system complexity and cost increase as well. This is mainly caused by the proportionally increase in the number of components such as filters that are needed to shape the Gaussian pulse. Recently, photonic-generation schemes aiming at increasing power efficiency of IR-UWB pulses have been reported in [24]–[28]. However, these photonic schemes are either complex or expensive especially for short-range fiber communication applications. Our approach utilizes the linear combination of lowest possible order derivative of Gaussian pulse, which has the potential of being simple and cheap. Hence, it is suited for short-range fiber communication networks in which complexity and cost are major issues.

B. Radiation Efficiency

As antennas are not efficient at low frequencies, the UWB pulses with low frequency or DC components cannot be used [7]–[9]. It is shown that the conventional pulses are good candidate waveforms in terms of radiation efficiency because they do not have a DC component. However, most of their energy lies in low frequencies. Similar to the conventional pulse, the designed pulse does not have a DC component as can be easily observed in Fig. 5. Furthermore, unlike the conventional pulse, most of the energy of proposed pulse as shown in Fig. 5 occupies higher frequency regions within the regulation mask. Hence, our pulse design together with pulse design techniques reported in [24]–[28] can achieve a relatively good radiation efficiency compared to the conventional pulse reported in [14]–[23].

C. Compliance With FCC Mask

UWB signal spectrum is one of the major issues confronting the industry and governments for commercial use. UWB systems cover a large spectrum and interfere with other existing wireless services. In order to keep this interference to a minimum, the FCC and other regulatory groups specify spectral masks for different applications, which allow power output for specific frequencies [7]–[9]. In Fig. 1, an example is shown of the FCC spectral mask for indoor UWB systems. A large contiguous bandwidth of 7.5 GHz is available between 3.1 and 10.6 GHz at maximum power output of -41.3 dB ·m/MHz. The major reason for extremely low allowed power output in the frequency bands 0.96–1.61 GHz is due to the pressure from groups representing existing services such as mobile telephony, GPS, and military usage [7]. This causes the primary concern in UWB communication due to electromagnetic interference between UWB systems and GPS band. Hence, from this viewpoint, the conventional monocycle and doublet pulses reported in [14]–[23] are not suitable for UWB transmission with good power efficiency. However, the pulse design techniques reported [24]–[28] and our proposed pulse are fully FCC compliant even in severely power-restricted area around GPS band as shown in Fig. 5 with significant improvement in power efficiency.

D. Power Efficiency

The FCC spectral mask limits the maximum permissible radiated power by the transmit antenna in UWB systems; that is, the effective isotropic radiated power must remain below the specified spectral mask. Compared to more conventional (narrowband) systems, pulse-shaping techniques can be used to optimize the greatest legally allowed transmission power to enhance power-limited IR-UWB systems [25]. The conventional pulses

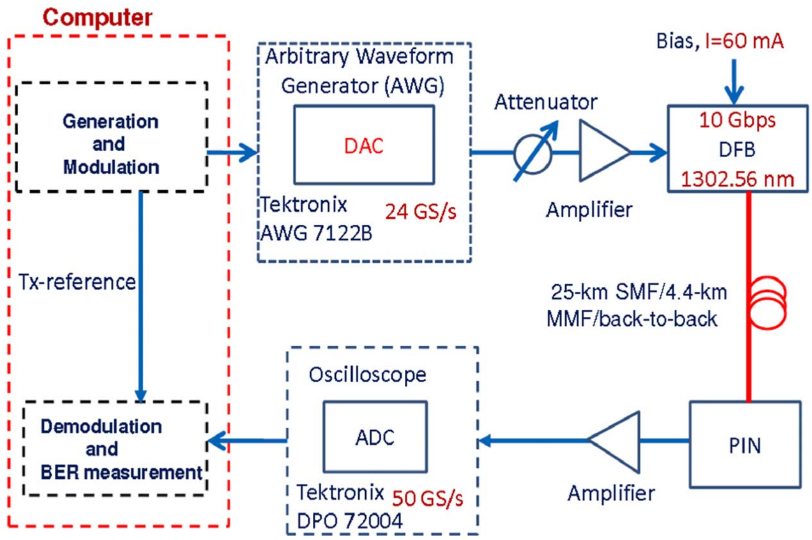

Fig. 6. Experimental setup.

based on monocycle and doublet used in [14]–[23] are not power efficient while forced to respect the FCC-mask requirements especially in the GPS band [25]. Based on the work done in [25], monocycle and doublet have a low power efficiency of 0.12% and 1.38%, respectively. To overcome the power inefficiency of these conventional pulses, power-efficient pulses based on photonic generation were reported in [25]–[28]. A photonic generation of IR-UWB with power efficiency of 63.6% was achieved in [26]. Very recently, a photonic generation with power efficiency of 50.97% was reported in [28]. However, in our approach, we use electrical generation that employs the conventional pulse together with some processing in order to increase the power efficiency. Accordingly, we have achieved a power efficiency of 48.52% which is a quite significant improvement over the conventional pulses reported in [14]–[23]. Although the power efficiency is less than the reported results in [25]–[28], we believe that the power efficiency can be increased further employing photonic generation at the expense of increasing complexity (and hence costs) in the system.

V. Experimental Setup

In order to realize high-speed IR-UWB over fiber for access and in-building networks application, the experimental setup depicted in Fig. 6 is used. The proposed IR-UWB pulse modulated by on–off keying (OOK) modulation using pseudorandom binary sequence (PRBS) of $2^{13} - 1$ data is constructed off-line in MATLAB. The modulated pulse is sent to a Tektronix arbitrary waveform generator (AWG 7122B) with a bandwidth of 10 GHz, running at 24 GSamples/s. To achieve this sampling speed, the two outputs ports of the AWG are interleaved. The DFB laser, with a wavelength of 1302.56 nm, is specified for up to 10 Gb/s OOK transmission and has an electrical small-signal modulation bandwidth of approximately 12 GHz. The biasing current is set at 60 mA in order to maintain the peak- to-peak current swing caused by generated IR-UWB fully lies in the linear portion of the *P–I* characteristics of the DFB. The resulting intensity-modulated optical signal is either transmitted over 25 km SMF or 4.4 km MMF during transmission case or directly coupled to optical attenuator in the back-to-back measurement case. After the optical attenuator, the received optical signal is detected by a 25 GHz MMF-coupled photodetector (New Fcous 1414 PD) with a photosensitive area of 24 μm and an integrated coupling lens. The received electrical signal is then amplified and captured using a 20 GHz real-time Tektronix DPO72004 digital storage oscilloscope running at a sampling rate of 50 GSamples/s for measuring the time-domain waveform and collect data for off-line processing such as demodulation and BER measurements. Finally, an RF spectrum analyzer is employed to present the electrical spectrum of our pulse and compare it to the FCC-mask requirement.

For the IR-UWB transmission, a computer is used for the digital IR-UWB modulation and demodulation in MATLAB, as shown in Fig. 6. This also includes off-line synchronization, evaluation of transmission performance such as BER measurement.

In general, in this paper, we consider the pulse design step which is before the real electronic demonstration. As a proof of concept, in the experimental demonstration, the UWB pulses were generated electronically using an AWG, which acts a digital-to-analog converter. Therefore, the output of AWG is a real electrical waveform of the combined pulse presented in (3). However, for a practical realization, an electrical signal generator that is dedicated to produce the designed pulse can replace the AWG. This electrical signal generator can be implemented using different options such as monocycle pulse generator together with wideband RF splitter and combiner, directly using a pulse synthesizer and digital CMOS circuitry.

VI. Experimental Results and Discussions

A. IR-UWB Over Optical Back-to-Back

Several modulation formats can be used for IR-UWB communication [7]–[9]. Recently, a comprehensive study on the implementation of multiple modulation schemes in IR-UWB over fiber system has been reported in [29]. A general theoretical

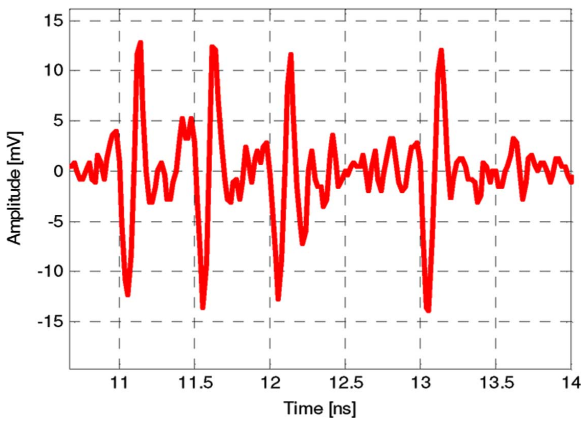

Fig. 7. IR-UWB pulse sequence in optical back-to-back.

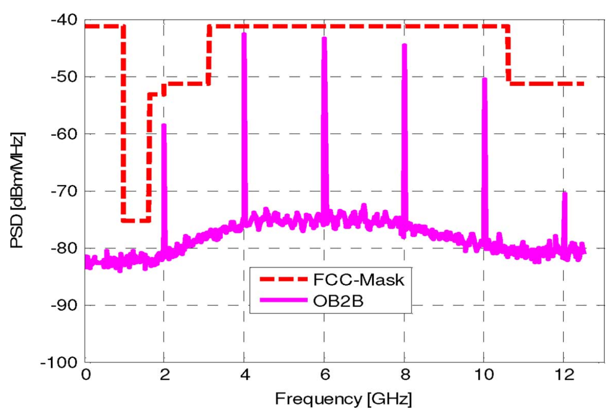

Fig. 8. PSD of IR-UWB pulse during optical back-to-back.

model to analyze the PSD of IR-UWB signals was developed to investigate the transmission performance of different modulation formats in [30]. However, OOK modulation of PRBS $2^{13}-1$ pattern length is used for simplicity and low-cost implementation. Fig. 7 shows some part of the transmitted data taken during the optical back-to-back measurement and clearly shows the OOK modulation of a binary sequence of 6 bits "**1 1 1 0 1 0**." Notice that we use ac-coupled amplifier in the detection part of experimental setup as shown in Fig. 6, which removes the dc part of the detected signal. Hence, both the negative and positive parts of the designed pulse is observed in Fig. 7. The spectrum of our generated IR-UWB is fully compatible with FCC mask, which has a central frequency of 6 GHz and a 10 dB bandwidth of 7.5 GHz is shown in Fig. 8. Notice that the spectrum shown in Fig. 8 has both continuous and discrete spectral components. The discrete spectral lines are called comb lines. These spectral lines appear on the top of continuous spectrum when repetitive pulses analyzed using an electrical spectrum analyzer (ESA). When repetitive pulses further amplitude modulated using OOK modulation type, the continuous part of the spectrum gets reduced and the spectral lines becomes more dominant. This is due to the slow response (thus averaging) in the ESA since there are more time slots in which no pulse generated. Furthermore, similar results of PSD have been reported [7]–[9] and even in very recent publications [27]–[30]. The comb lines appear at the locations that are the multiples of the inverse of the pulse repetition interval. Hence, in this case, they appear at multiples of

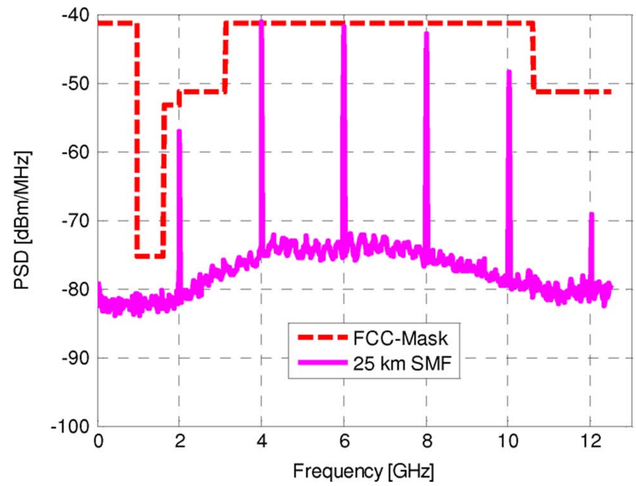

Fig. 9. PSD of IR-UWB after 25 km SMF fiber.

2 GHz which is exactly equal to the bit rate of the transmission system. These spectral lines are not favorable regarding the FCC mask and the interference that can be made to other operating wireless systems. Hence, the comb lines are undesirable as they limit the total transmit power. One method to reduce the spectral lines of the UWB signal is to use randomly delayed pulse position modulation [8]. In our case, the comb lines are forced to remain below the FCC mask in order to avoid interference to other operating wireless systems. Finally, the results depicted both in a time and frequency domain as in Figs. 7 and 8 confirm that the signal is not distorted during the optical back-to-back case. This is mainly due to the system bandwidth that is adequate enough for the signal bandwidth.

B. IR-UWB Over SMF for Access Networks

SMF offers a very wide bandwidth, very low attenuation and high linearity [31]. IR-UWB over SMF fiber could be an attractive solution for the distribution of high-definition audio and video content in fiber-to-the-home networks [32]. However, the relative high cost of UWB over SMF fiber is attributed to the cost of optical transceivers. To lower the cost of IR-UWB over SMF, the IR-UWB signal processing can be centralized in order to simplify IR-UWB base stations [31]. In the cheapest case, an intensity-modulated direct-detection (IM-DD) system is employed for the IR-UWB transceiver. Therefore, in the experiment shown in Fig. 6, we employ the IM-DD technique using a directly modulated high-speed DFB and a standard SMF used in the experiment. After 25 km SMF transmission, the PSD of the pulse is shown in the Fig. 9. The results clearly show the successful transmission of 2 Gb/s without any significant distortion in the frequency domain mainly due to near-zero dispersion at 1300 nm and high transmission capacity of the SMF fiber.

C. IR-UWB Over MMF for In-Buildings Networks

Silica MMF with core diameter of 50 to 62.5 μm is attractive for use a high-capacity and low-cost optical fiber-based links in local area networks, such as enterprise in-building and datacenter backbones, but also short-distance server/computer interconnects. In contrary to long-haul transmission links, silica MMF is used for the vast majority of optical local area network

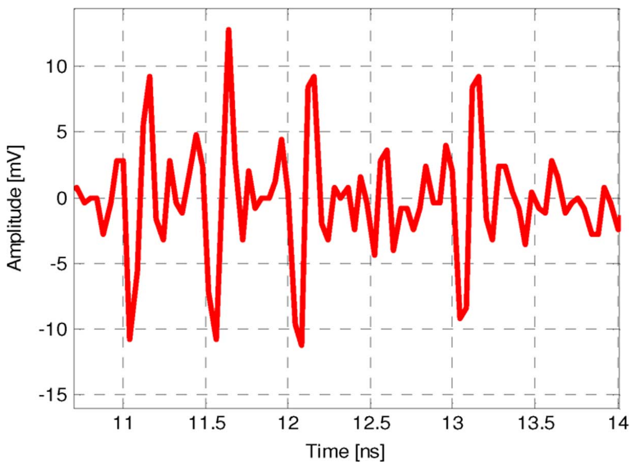

Fig. 10. IR-UWB pulse sequence after 4.4 km MMF fiber.

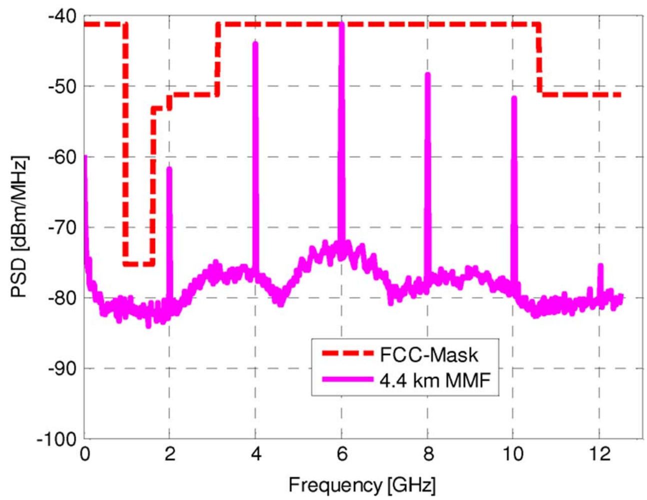

Fig. 11. PSD of IR-UWB over fiber after 4.4 km MMF fiber.

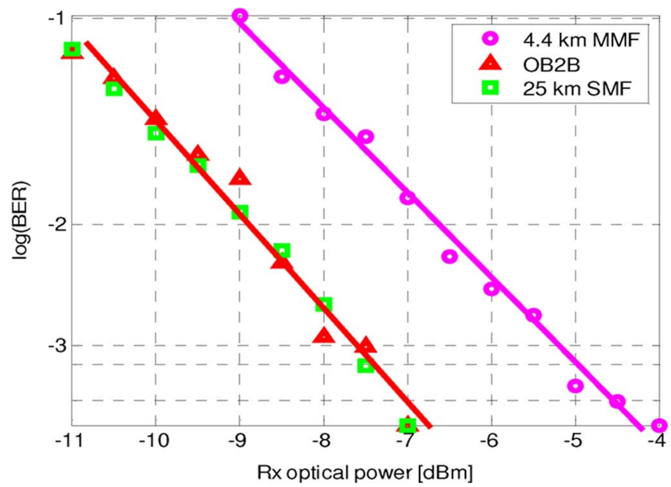

Fig. 12. BER curves for optical back-to-back, 25 km SMF, and 4.4 km MMF.

links. Unlike SMF, the large core diameter of the MMF allows large alignment and dimensional tolerance in transceiver components, thereby lowering installation, maintenance, and component cost [33]. Therefore, IR-UWB over MMF is an attractive solution for in-building networks applications. The MMF from Draka Comteq fiber used in this experiment has a high numerical aperture with bandwidth length product of 8925 MHz.km and a loss of 0.45 dB/km at 1300 nm, which allows the transmission of 2 Gb/s IR-UWB over 4.4 km MMF without severe distortion. The time-domain waveform is shown in Fig. 10. There is no significant degradation after 4.4 km MMF transmission; Fig. 11 finally shows the spectrum of the received IR-UWB signal after 4.4 km MMF transmission. The signal spectrum is still very nicely fitting into FCC mask with very small periodical notch observed in the spectrum, which signify the mode coupling leading to interference between guided mode and other modes, which are delayed with respect to its own signal.

D. BER Performance of IR-UWB Over SMF and MMF

Fig. 12 shows the BER results of 2 Gb/s IR-UWB signal transmissions over 25 km SMF, 4.4 km MMF, and optical back-to-back case. For each BER measurement points, 8191 bits following a $2^{13} - 1$ PRBS pattern are transmitted and recorded using a 50 GSamples/s digital oscilloscope. The BER is subsequently computed using a DSP algorithm in a bit-for-bit comparison between the transmitted and received data. The DSP algorithm distinguished between binary "1" and "0" by comparing the average power within the central window of each bit slot to an adaptive decision threshold. This approach is expected to provide more accurate results than BER estimates from the eye diagram Q-factor as in [32]. According to the result of the BER measurement, the 4.4 km MMF transmission shows a penalty of almost 3 dB due to the combined effect of intermodal dispersion, mode mixing, and modal noise at the receiver side. However, for the 25 km SMF transmission no penalty is observed. This is mainly due to the high-capacity and low-signal dispersion around 1300 nm. In general, the experimental result shows a successful transmission within the forward error free (FEC) limit of IR-UWB over both 25 km SMF and 4.4 km MMF for both access and in-building applications.

VII. Conclusion

We have theoretically investigated and experimentally demonstrated a simple IR-UWB pulse-generation technique by linearly combining two monocycles using different pulse-shaping factors. The generation technique has potentially low complexity and hence low cost compared to higher order Gaussian derivative generation techniques. The proposed pulse has many features such as high power efficiency, high spectral efficiency, and good radiation efficiency compared to the conventional monocycle and doublet pulses. Furthermore, the pulse has a fractional bandwidth of 125% and fully complies with the FCC-indoor spectrum mask even in the most severely power-restricted GPS band from 0.96 to 1.61 GHz. We also experimentally investigated the performance of IR-UWB over fiber using off-line BER evaluation. Accordingly, we achieved an FEC-limit error-free transmission of 2 Gb/s IR-UWB over 25 km SMF and 4.4 km MMF. We believe that our newly proposed IR-UWB over fiber has a potential application in low-cost high-speed short-range communication networks.

References

[1] G. R. Aiello and G. D. Rogerson, "Ultra-wideband wireless systems," *IEEE Microw. Mag.*, vol. 4, no. 2, pp. 36–47, Jun. 2003.

[2] R. Jafari and K. Gilani, "Body sensor networks and ultra wideband communication," *ICUWB2008*, vol. 3, no. 2, pp. 9–10, 2008.

[3] J. Yao, "Photonics for ultra wideband communications," *IEEE Microw. Mag.*, vol. 4, no. 2, pp. 82–495, Jun. 2009.

[4] M. G. Di Benedetto and B. Vojcic, "Ultra-wideband wireless communications: A Tutorial," *J. Commun. Netw.*, vol. 5, no. 4, pp. 290–302, Dec. 2003.

[5] W. P. Lin and J. Y. Chen, "Implementation of a new ultrawideband impulse system," *IEEE Photon. Technol. Lett.*, vol. 17, no. 11, pp. 2418–2420, Nov. 2005.

[6] X. Chen and S. Kiaei, "Monocycle shapes for ultra wideband system," in *IEEE Int. Symp. Circuits Syst.*, May 2002, vol. 1, pp. 26–29 .

[7] M. Ghavami, L. B. Michal, and R. Kohno*, Ultra WideBand Signals and Systems in Communication Engineering*. West Sussex, England: Wiley, 2007 .

[8] H. Nikookar and R. Prasad, "Introduction to ultra wideband for wireless communications," in *Springer Science and Business Media*. New York: Springer-Verlag, 2009.

[9] M. Gabriella and G. Giancola*, Understanding Ultra Wideband Radio Fundamentals*. Upper Saddle River, NJ: Pearson Education, Inc., 2004.

[10] H. Sheng, "On the spectral and power requirements for ultra wideband transmission," in *IEEE Int. Conf. Commun. (ICC)*, May 2003, vol. 1, pp. 738–742 .

[11] B. Parr, B. Cho, K. Wallace, and Z. Ding, "A novel ultra-wideband pulse design algorithm," *IEEE. Commun. Lett.*, vol. 7, no. 5, pp. 219–221, May 2003.

[12] N. C. Beaulie and B. Hu, "A pulse design paradigm for ultra-wideband communication systems," *IEEE Trans. Wireless Commun.*, vol. 5, no. 6, pp. 1274–1278, Jun. 2006.

[13] B. Allen, S. Ali Ghorashi, and M. Ghavami, "A review of pulse design for impulse radio," in *Proc. UWB Commun. Technol. Syst. Des.*, Jul. 2004, pp. 93–97.

[14] J. Yao, F. Zeng, and Q. Wang, "Photonic generation of ultrawideband signals," *J. Lightw. Technol.*, vol. 43, no. 2, pp. 3219–3235, Nov. 2007.

[15] J. D. McKinney and A. M. Weiner, "Shaping the power spectrum of ultra-wideband radio-frequency signals," *IEEE Trans. Microw. Theory Tech.*, vol. 54, no. 12, pp. 4247–4255, Dec. 2006.

[16] C. Wang, F. Zeng, and J. P. Yao, "All-fiber ultrawideband pulse generation base on spectral shaping and dispersion-induced frequency-to-time conversion," *IEEE Photon. Technol. Lett.*, vol. 19, no. 3, pp. 137–139, Feb. 2007.

[17] F. Zeng and J. Yao, "An approach to ultrawideband pulse generation and distribution over optical fiber," *IEEE Photon. Technol. Lett.*, vol. 18, no. 7, pp. 823–825, Apr. 2006.

[18] F. Zeng and J. Yao, "Ultra-wideband impulse radio signals generation using a high-speed electrooptic phase modulator and a fiber-Bragg-grating—based frequency discriminator," *IEEE Photon. Technol. Lett.*, vol. 18, no. 19, pp. 2062–2064, Oct. 2006.

[19] Q. Wang and J. P. Yao, "Optically switchable UWB monocycle and doublet generation using a reconfigurable photonic microwave delay line filter," *Opt. Exp.*, vol. 15, no. 22, pp. 14667–14672, Oct. 2007.

[20] Q. Wang, F. Zeng, S. Blais, and J. P. Yao, "Optical ultrawideband monocycle pulse generation based on cross-gain modulation in a semiconductor optical amplifier," *Opt. Lett.*, vol. 31, no. 21, pp. 3083–3085, Nov. 2006.

[21] H. Chen, M. Chen, T. Wang, M. Li, and S. Xie, "Methods for ultra-wideband pulse generation based on optical cross-polarization modulation ," *J. Lightw. Technol.*, vol. 26, no. 5, pp. 2492–2499, Aug. 2008.

[22] J. Li, S. Fu, K. Xu, J. Wu, J. Lin, M. Tang, and P. Shum, "Photonic ultrawideband monocycle pulse generation using a single electro-optic modulator ," *Opt. Lett.*, vol. 33, no. 3, pp. 288–290, Feb. 2008.

[23] S. L. Pan and J. P. Yao, "An optical UWB pulse generation for flexible modulation format," *IEEE Photon. Technol. Lett.*, vol. 21, no. 19, pp. 1381–1383, Sep. 2009.

[24] M. Bolea, T. Mora, B. Ortega, and J. Capmany, "Optical UWB pulse generator using an N tap microwave photonic philter and phase inversion adaptable to different modulation formats," *Opt. Exp.*, vol. 17, no. 7, pp. 5023–5032, Mar. 2009.

[25] M. Abtahi, J. Magne, M. Mirshafiei, L. Rusch, and S. LaRochelle, "Generation of power-efficient FCC-compliant UWB waveforms using FBGs: Analysis and experiment ," *J. Lightw. Technol.*, vol. 26, no. 5, pp. 628–635, Mar. 2008.

[26] M. Abtahi, M. Mirshafiei, S. LaRochelle, and L. A. Rusch, "All-optical 500-Mb/s UWB transceiver: An experimental demonstration," *J. Lightw. Technol.*, vol. 26, no. 15, pp. 2795–2802, Aug. 2008.

[27] E. Zhou, X. Xu, K. Lui, and K. K. Wong, "Power-efficient ultra-wideband pulse generator based on multiple PM-IM conversions," *IEEE Photon. Technol. Lett.*, vol. 22, no. 14, pp. 1063–1065, Jul. 2010.

[28] E. Zhou, X. Xu, K. Lui, and K. K. Wong, "High-speed photonic power-efficient ultra-wideband transceiver based on multiple PM-IM conversions ," *IEEE Trans. Microw. Theory Tech.*, vol. 58, no. 11, pp. 3344–3351, Nov. 2010.

[29] S. L. Pan and J. P. Yao, "UWB-over-fiber communications: Modulation and transmission," *J. Lightw. Technol.*, vol. 28, no. 16, pp. 2445–2455, Aug. 2010.

[30] S. L. Pan and J. P. Yao, "Performance evaluation of UWB signal transmission over optical fiber," *IEEE. J. Sel. Area Commun.*, vol. 28, no. 6, pp. 899–900, Aug. 2010.

[31] Y. Le Guennec, M. Lourdiane, B. Cabon, G. Maury, and P. Lombard, "Technologies for UWB over fiber," in *Proc. IEEE Lasers Electro-Opt.*, Oct. 2006, pp. 518–519.

[32] R. Llorente, T. Alves, M. Morant, M. Beltran, J. Perez, A. Cartaxo, and J. Marti, "Ultra-wideband radio signals distibution in FTTH networks," *IEEE Photon. Technol. Lett.*, vol. 20, no. 11, pp. 945–947, Jun. 2008.

[33] T. Koonen, H. van den Boom, and G. D. Khoe, "Broadband access and in-house networks: Extending the capabilities of multimode fiber networks ," in *Proc. Eur. Conf. Optical Commun. (ECOC)*, 2003, pp. 24–27.

Solomon Tesfay Abraha (S'09) was born in Ethiopia in 1979. In 2003, he received the B.Sc. degree (with very great distinction) in electrical engineering with specialization of communication technology in Ethiopia. In 2006–2008, he received Netherlands Fellowship Program scholarship grant from Delft University of Technology (TU Delft), The Netherlands. In 2008, he received the M.Sc. degree in telecommunications engineering from TU Delft. In the same year, he joined COBRA Research Institute at Eindhoven University of Technology in The Netherlands. He is currently doing research on European Union FP7 program ALPHA project toward the Ph.D. degree in the field of Impulse Radio Ultrawideband over fiber.

Chigo Okonkwo (S'04–M'09) received the B.Eng., M.Sc., and Ph.D. degrees from the University of Essex, Essex, U.K., in 2001, 2002, and 2009, respectively.

In 2004, he joined the Photonic Networks Research Laboratory, University of Essex as a Senior Research Officer working on UK EPSRC funded research projects. In 2009, he was appointed as a Senior Researcher at the COBRA Research Institute, Eindhoven University of Technology, Eindhoven, The Netherlands. His contributions are on all-optical signal processing and plastic optical fiber systems for access and in-building networks within European Union FP7 research projects ALPHA, POF-PLUS, and EURO-FOS.

Hejie Yang (S'07) was born in Tianjin, China, in 1982. He received the M.Sc. degree in telecommunications from the Technical University of Denmark, Copenhagen, Denmark, in 2006, and the Ph.D. degree in the area of future home network from COBRA Research Institute, Eindhoven University of Technology, Eindhoven, The Netherlands, in 2011.

Since February 2011, he has been involved in applied research at Corning Incorporated, Corning, NY.

Davide Visani (S'09) was born in Faenza, Italy, in 1984. He received the B.Sc. and M.Sc. degrees in telecommunications from the University of Bologna, Bologna, Italy, in 2006 and 2008, respectively. He is currently working toward the Ph.D. degree in optical fiber technologies and radio over fiber for in-building and in-home networks at the Dipartimento di Elettronica Informatica e Sistemistica (DEIS), University of Bologna.

In 2010, he spent a year working at the COBRA Research Institute, Eindhoven University of Technology, Eindhoven, The Netherlands.

Yan Shi (S'10) received the M.Sc. degree in engineering electronic science and technology from Zhejiang University, Hangzhou, Zhejiang, China, in 2008. She is currently working toward the Ph.D. degree in the COBRA Research Institute, Eindhoven University of Technology, Eindhoven, The Netherlands. She is performing her research on the EU projects POF-PLUS and EURO-FOS.

Her current research interests include ultrawideband signals communication over plastic optical fiber for short-reach applications.

Hyun-Do Jung (M'00) received the B.S. degree in radio sciences and engineering from Kyung Hee University, Seoul, Korea, in 1999, and the M.Sc. and Ph.D. degrees in electrical and electronic engineering from Yonsei University, Seoul, Korea, in 2005.

From 2005 to 2010, he was with the Eindhoven University of Technology, Eindhoven, The Netherlands, as a Postdoctoral Researcher on the topic of optical packet switching and reconfigurable access networks. Since 2010, he has been with the Bell Labs Seoul, Alcatel-Lucent, Seoul, Korea as a member of technical staff. His current research interests include mm-RoF technologies, optical access networks, and optical packet switching.

Eduward Tangdiongga (S'01–M'10) received the M.Sc. and Ph.D. degrees from the Eindhoven University of Technology, Eindhoven, The Netherlands, in 1994 and 2001, respectively.

In 1994, he joined the COBRA Research Institute. From 2001 to 2006, he participated in the EU FP5 IST-FASHION and the Dutch STW research project on ultrahigh-speed optical switch using semiconductor materials. In 2006, he was appointed as an Assistant Professor on short-haul optical communications. Currently, he is involved in European Union FP7 research programs ALPHA, POF-PLUS, BOOM, and EUROFOS. His research interest includes radio over fiber and plastic optical fiber.

Ton Koonen (M'00–SM'01–F'07) is a Full Professor at Eindhoven University of Technology (TU/e), Eindhoven, The Netherlands, since 2001, and the Chairman of the group Electro-Optical Communication Systems since 2004. Before joining TU/e, he worked for more than 20 years in applied research in industry, a.o. at Bell Laboratories in Lucent Technologies, and as a Part-Time Professor at Twente University.

Prof. Koonen is a Bell Labs Fellow, and he was an elected member of the IEEE Photonic Society Board of Governors. He is involved in many European research projects, both as participant and as reviewer. His current research interests include optical fiber access and in-building networks, including radio-over-fiber techniques.